International Journal of Recent Advances in Multidisciplinary Topics
Volume 6, Issue 2, February 2025
https://www.ijramt.com | ISSN (Online): 2582-7839

A Detailed Analysis of Star Formation and AGN Feedback Mechanism in Spiral Galaxy

Rihana Abdul Kabeer[1*], Shana Mariyam[2]
[1,2]*Physics Teacher, Department of Physics, Ministry of Education, Dubai, UAE*

***Abstract*: The manners in which stars form as well as how the Star Formation (SF) method is regulated in galaxies are the main themes in extragalactic astronomy. The SF analysis was examined by several prevailing researchers. But star formation in the cosmic environment with radiative and mechanical Active Galactic Nucleus (AGN) feedback mechanisms wasn't investigated in most of the prevailing research works. A detailed analysis of SF and AGN feedback mechanisms in spiral galaxies is propounded in this paper. Assessing star formation and determining whether the feedback mechanism's effect is positive or negative in spiral galaxies are the research's main objectives. Moreover, this research analysis considers the J0313–1806 astronomical data for covering the cosmic environment in the SF of the spiral galaxy. For assessing the atomic, molecular, and Diffused Ionized Gas (DIG) values, hydrodynamic analysis is carried out. By utilizing the Silk-Elmegreen law, the relationship betwixt the Star Formation Rate (SFR) and the surface density of gas during SF in a spiral galaxy is assessed. According to the experimental results, the DIG has a higher fractional contribution, and the AGN feedback mechanism provides a positive effect on star formation.**

***Keywords*: Active Galactic Nucleus, (AGN) Feedback, Diffuse Ionized Gas (DIG), Radiative mechanism, Star Formation Rate (SFR), Silk-Elmegreen Law, Spiral Galaxies.**

1. Introduction

A vital evolution in the total galaxy population was exposed by galaxy population works at a low to intermediate redshift of z ∼2 over the past 2 decades (Tuttle & Tonnesen, 2020). Prevailing works presented several research studies that assessed the evolutionary pathways from the star-forming galaxies' blue cloud to quiescent galaxies' red sequence (Guo et al., 2020). Moreover, for star formation, various models like stellar feedback, the chemistry of the Interstellar Medium (ISM), as well as thermodynamics were utilized in the previous years (Semenov et al., 2021). The ISM that had different limitations for continuous energy input modeling stellar wind sources includes the expansion of the H II region (Ostriker & Kim, 2022). The observation exhibits that the surface density of SF is well correlated with the molecular gas's surface density. This empirical correlation's physical interpretation is that low gas temperatures as well as high densities occurring in ISM's co-spatial locations are needed for both SF and molecular hydrogen formation (Feldmann, 2020). Star Clusters (SCs) consist of thousands of stars that are formed by fragmentation of molecular gas into massive clouds, which consecutively collapse the critical mass, gas temperature, as well as density required to trigger SF (Prieto et al., 2024). By using the acquisition and distribution of angular momentum, the star's structure and kinetic energy are determined (Zhou et al., 2021). The galaxy's Rotation Curve (RC) is very essential since it provides valuable information regarding the united distribution of baryonic as well as dark matter in galaxies (Frosst et al., 2022). In a spiral galaxy, spiral arms are of dominant significance in disk galaxies' chemical and dynamical evolution (Kim et al., 2020). Prevailing research works related to star formation in galaxies propounded several observational data (Fraser-McKelvie et al., 2020). Nevertheless, the analysis of star formation lacked some details. Thus, a detailed analysis of star formation as well as radiative and mechanical AGN feedback in spiral galaxies with cosmic environment is presented in this research approach.

A. Problem Statement

A few issues in prevailing research works are described below:

- In most of the prevailing research works, the star formation of spiral galaxies in a cosmic environment wasn't covered.
- In prevailing (Yu et al., 2021), a limited number of factors were considered, thus affecting the investigation result.
- Existing (Calura et al., 2022) didn't assess the relationship betwixt SFR and surface gas density, thus affecting the clump identification and segmentation process.
- Most of the existing research works analyzed a smaller number of samples for star formation, which cannot support large-scale galaxy samples.

B. Objectives

The propounded research has some objectives, which are given here:

- The analysis is carried out by data collection from J0313–1806 astronomical data of spiral galaxies with cosmic environment.
- The research analyzed the atomic, molecular, and DIG.
- For evaluating the relationship between the star

*Corresponding author: rihaaa265@gmail.com

formation by utilizing Silk-Elmegreen law.

- To assess the star formation by large-scale galaxy samples in J0313–1806.

The presented research article's structure is given as: The prevailing research investigations centered on star formation are presented in Section 2, Section 3 describes the background of the SF and the theories, in Section 4, the detail of observational data is given, section 5 assesses the experimental outcome, and the article is concluded with future development in section 6.

2. Related Work

(Aouad et al., 2020) assessed spatially resolved kinematics along with the SFR density using the combined model of 17 nearby spiral galaxies. Here, the neutral hydrogen radio observation as well as multi-wavelength spectral energy distribution study was utilized. Investigational assessment displayed that the Oort parameters were proportional to the overall kinetic energy of collisions. The empirical analysis exhibited how the galaxy's overall SFR was distributed via the disc. But the analysis was held only with less number of samples. (Yu et al., 2021) examined the impact of spiral structure boosts SF in disk galaxies. Primarily, the relationship betwixt various factors of SF like spiral arms, stellar mass, and SFR was assessed. Experimental assessment showed that arm strength was positively correlated with the mass function. As per the overall outcome, the arm strength was elevated with shorter gas depletion time. Nevertheless, the work assessed only the strength between the star formation factors; however, other star formation factors weren't assessed. (Nesvadba et al., 2021) propounded a arcsecond-resolution Atacama Large Millimeter Array (ALMA) CO (1−0) interferometry to examine the star formation. For the SFR, the Galaxy Evolution Explorer and Wide-Field Infrared Survey Explorer (WISE) were utilized. Here, for explaining the low SFR, the radio AGN feedback was utilized. As per the work's experimental assessment, considerable offsets toward low SFR densities were also established for the Silk-Elmegreen relationship as well as extended Schmidt-law. But all factors like halo gas weren't covered, which affected the research's reliability. (Valentini et al., 2023) analyzed the H2 modelling as well as the description of stellar feedback in low-metallicity environments. Here, for estimating gold gas's molecular fraction, theoretical and phenomenological prescription models were employed. The propounded research work yielded superior outcomes in observing nearby disc galaxies. But an issue might be represented by the adoption of model star formation in cosmological simulations through observations of nearby galaxies.

(Rieder et al., 2022) recommended an approach to simulate SCs from birth in a live galaxy simulation. Here, for simulating star as well as SC formation in spiral arms, the Smoothed Particle Hydrodynamics (SPH) technique PHANTOM with the N-body technique PETAR was utilized. Firstly, the regions were chosen after the selection of regions from pre-run simulations. Next, to obtain a higher resolution, the particles were re-sampled. Investigational assessment evaluated the early evaluation of the embedded SCs in the regions. Yet, all the factors of star formation weren't covered in the work, which diminished the star formation analysis. (Lammers et al., 2023) reconstructed the non-parametric SF histories in spatially resolved spaxels that cover each galaxy's face. Here, the AGN feedback was utilized. Moreover, the control galaxies that provided AGN feedback's direct observational evidence to suppress SF were considered. As per the experimental outcome, the AGN feedback considerably affected the central star formation. However, the AGN feedback was ineffective in the driving galaxy-wide quenching in low-redshift galaxies. (Calura et al., 2022) established a set of zoom-in cosmological simulations with a sub-pc resolution for star formation. Here, the stochastic and mass functions were utilized to generate massive stars. For preventing the artificial radiative loss of the energy injected by individual stars in very dense gas, the work utilized the modified 'delayed cooling' feedback scheme. The investigational outcome exhibited star formation occurred in dense gas clumps lying at the centers of networks of cold, low-pressure, and elongated filaments with surface densities. Yet, the work didn't discuss the problems of clump identification and segmentation regarding the relationship analysis. (Calura et al., 2022) propounded the observational analysis for assessing the early star formation in proto-spiral galaxies. The analysis was done with density evolution, SFR, masses, and sizes. According to the outcome analysis, the galaxies signified the foremost mode of SF in the early universe. But the acquired outcome might be unreliable since the analysis was done with low spatial-resolution data. (Gillman et al., 2020) indicated a study of the gas dynamics of SF galaxies at $z \sim 1.5$. By utilizing parametrical and non-parametrical images of galaxies, the analysis was carried out. Here, the relationship betwixt stellar-specific angular momentum and stellar mass were assessed. According to the experimental outcome, the $j* - M*$ plane was strongly correlated with the SF surface density. But the star formation analysis didn't analyze the correlations well. (Smith et al., 2021) established the radial, local, and global photometric assessment of star formation. Here, the double exponential Star Formation History (SFH) was utilized for the assessment. The experimental assessment presented a stronger relationship during SF. But the discernible difference in the relationship assessment wasn't considered.

3. Background and Theories to Assess the Structure of Spiral Galaxy

By using Density-Wave (DW) theory, spiral galaxies' structure and dynamics are assessed. The spiral density waves' presence in galaxies has implications for star formation. The density wave theory exposes that the spiral arms don't contain the same gas clouds as well as stars continually. The spiral arms at any moment indicate the local maxima of a DW in the galaxy. The DW is caused as well as maintained by purely gravitational effects, not by pressure variations. Thus, the DWs in galaxies are completely dissimilar from ordinary sound waves that are pressure-supported. For assessing the spiral arms, rival theories are utilized. It is defined that the pitch angle shouldn't rely on

the wavelength. Disc galaxies don't rotate as solid bodies rather they rotate differentially. This rotation's consequence is categorized by 2 foremost physical effects, namely vorticity and shear, both of which are stated as functions of the angular frequency Ω (F) of the galactic rotation as well as the gradient of the angular frequency regarding the radius dΩ/dF. Initially, based on the total amount of stress betwixt the differentially rotating annuli, the galactic shear is derived. The total amount of stress $\wp$ is derived in equation (1).

$$\wp = -0.5\,F\frac{d\Omega}{dF} \tag{1}$$

Then, the shearing motion is derived in equation (2) as,

$$z = s\left(\Omega - \frac{dU}{dF}\right) \tag{2}$$

Here, z is the shear velocity, the radial separation betwixt 2 orbits is signified by s, and U is the relative velocity. Next, the galaxy's vorticity is derived by the second Oort parameter $\hbar$ and is given as,

$$\psi = \left|2\hbar\right| \tag{3}$$

Here, ψ is the vorticity. The second Oort parameter $\hbar$ is derived in equation (4) as,

$$\hbar = -\left(\Omega + 0.5\,F\frac{d\Omega}{dF}\right) \tag{4}$$

The epicyclic frequency ξ is measured from the rotation of the galaxy curve and expressed in equation (5) as,

$$\xi = \sqrt{-4\hbar\Omega} \tag{5}$$

While studying the stellar disks' stability, Toomre established that a rotating stellar disk was unstable ($\Re < 1$). Thus, the "Toomre parameter" $\Re$ is expressed as,

$$\Re = \frac{\xi\delta}{\pi R\Sigma} \tag{6}$$

Here, the velocity dispersion is specified by δ, R signifies the gravitational constant, as well as Σ is the gas surface density.

4. Observational Material

The spiral galaxy's structure is assessed according to the specified theories. The image data and photometric data are gathered for the assessment. The further section discusses the data collection as well as the analysis procedure of SF in spiral galaxies.

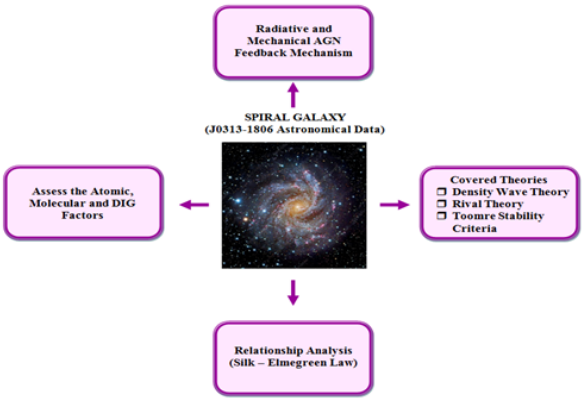

Fig. 1. Structure of the presented study

In Figure 1, the presented analysis's structure is exhibited.

A. Data

For the research framework, the data were gathered from J0313–1806, which was picked as a z > 7.2 quasar candidate from prevailing work (Yang et al., 2020). In January 2021, it was recognized as the most redshifted (highest z) known quasar, with the oldest known Supermassive Black Hole (SMBH) at $(1.6\pm0.4)\times10^9$ solar masses. It has an imaging dataset combining optical imaging from Pan-STARRS1 (Smartt et al., 2023), infrared imaging from the UKIRT Hemisphere Survey (Dye et al., 2018), the DESI Legacy Imaging Surveys (Xu et al., 2023), the VISTA Hemisphere Survey (Meingast et al., 2023), as well as the WISE survey (Jarrett et al., 2023). In the infrared bands, all the formation and feedback processes are detected. The J0313–1806 is a well-documented quasar with coordinates RA 03h 13m, Dec -18° 06′. z = 7.64 is the accurate redshift value of J0313–1806 astronomical data, and it is the most distant quasars known. This is incredibly luminous with bolometric luminosity around 2×10^{13} solar luminosities, as well as its high luminosity is a characteristic of early and massive quasars. This helps understand SMBHs' formation and growth as well as the conditions in the early cosmic epoch. The J0313–1806 data was widely studied with different observational approaches like radio, optical, and space-centric observations. These approaches centered on analysis contain detailed information regarding the properties of the objects, namely luminosity, host galaxy, and redshift. Moreover, it is more important because of its very high redshift, luminosity, as well as availability of detailed data. Here, the emissions during star formation are also evaluated. The emissions are molecular, ionized, and atomic gas.

B. ALMA Observations

The spiral galaxy's redshift and other properties are determined. Here, the detected J0313– 1806 with an ALMA in a C43-4 configuration is assessed. For calibrating the bandpass, phase, amplitude, as well as flux, the study utilizes the Common Astronomy Software Application (CASA) version 5.6 for reducing the data by implementing the automatic flagging of visibility.

C. AGN Feedback

To regulate star formation, control galaxy growth, shape galactic structure, modulate Black Hole (BH) growth, and influence galaxy morphology and dynamics, the AGN feedback mechanism assessed the gathered star formation of J0313–1806. Here, centered on the AGN feedback, the SF is examined. The combination of both radiative AGN and mechanical AGN is considered. The AGN feedback plays an essential role in the galaxies' evolution, especially in the situation of star formation. The AGN feedback systems significantly vary in their accretion rates as well as in their effects and feedback strength. In general, the AGN feedback models are centered on the Bondi accretion rate. It is the spherical accretion of a compact object traveling via the ISM, as well as it is mostly utilized in the context of a neutron star as well as BH accretion. The derivation for the Bondi accretion rate Acc_{bon} is expressed in equation (7).

$$Acc_{bon} = \frac{2\pi R^2 Z_{BH}^2 \sigma_s}{\left(\mu_s^2 + j^2\right)^{3/2}} \tag{7}$$

Here, the BH's mass is specified by Z_{BH} , the gas's density and sound speed at infinity are signified by σ_s and μ_s , correspondingly, as well as BH's speed in relation to the distant gas is indicated by j . A BH's mass is signified in 2 ways, namely the dynamic mass of the BH particle as well as the physical BH's "sub-grid-scale". The physical BH's "sub-grid-scale" mass is derived using the equation (7). The BH's dynamic mass is derived using the maximum accretion rate in spherically symmetric hydrodynamic equilibrium, and it is represented as Eddington accretion rate Acc_{edd} , which is arithmetically given in equation (8) as,

$$Acc_{edd} = \frac{4\pi R Z_{BH} \ell_p}{\omega_{rad} \varpi_{TCS}} \tag{8}$$

Here, the proton's mass is signified by ℓ_p , the radiative efficacy is specified by ω_{rad} , as well as the Thomson cross-section is denoted as ϖ_{TCS} . Lastly, the numerical accretion rate is derived in equation (9) as,

$$N_{acc} = \min\left(Acc_{edd}, \varepsilon Acc_{bon}\right) \tag{9}$$

Here, ε is the factor for the numerical accretion rate.

D. Star Formation Strength Assessment Methods

Here, the Silk-Elmegreen law examines the star formation strength of J0313–1806 and computes the relationship in astrophysics. It measures the maximum gas density for star formation to occur without being disrupted by internal pressure or other factors. The derivation for the Silk-Elmegreen law is expressed in equation (10).

$$\aleph_{\max} \approx \frac{\mu_s^2}{\pi R \kappa} \tag{10}$$

Where, the maximum gas surface density is symbolized by, $\aleph_{\max}$ as well as κ depicts the gas density.

5. Experimental Analysis

Here, by considering feedback and other factors, the star formation in a spiral galaxy is assessed.

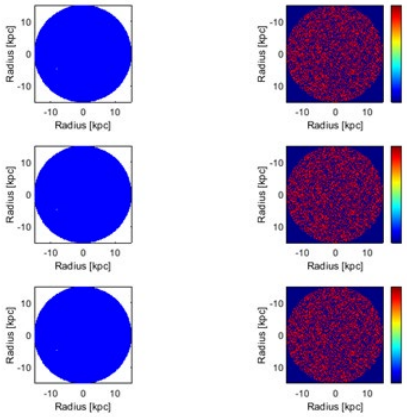

Fig. 2. The map structure of the optical imaging of spiral galaxy

The map structure for the spiral galaxy's optical imaging is displayed in Figure 2. The map helps determine the density of gas and stars. It exhibits the entire galaxies. Moreover, it is helpful to extract detailed information like vorticity, stress, epicyclic frequency, and other factors.

A. Hydrodynamic Analysis

During star formation, the interplay between the molecular, atomic, and ionized gases is essential. Here, all 3 factors are examined by considering a fractional contribution.

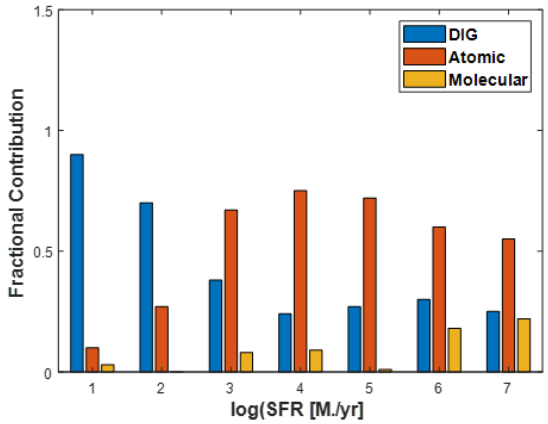

Fig. 3.

In Figure 3, the graphical plot for hydrodynamic analysis is displayed. This is useful to predict galaxies' luminosities. The hydrodynamic process simulation finds the relative contributions regarding the galaxy-averaged SFR. Here, the fractional contribution varied according to the SFR variation. DIG obtains the highest fractional contribution value. The

analysis exhibits that in the spiral galaxy, the DIG is higher.

B. Relationship Assessment

Here, for analyzing the complexity involved in how molecular clouds turn into stars, the relationship is evaluated during the star formation.

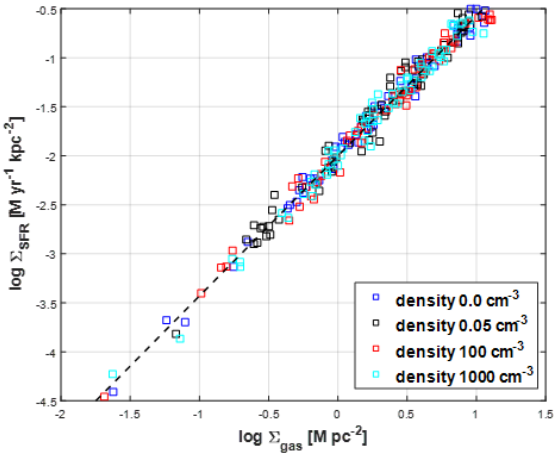

Fig. 4.

Figure 4 displays the relationship assessed during the star formation. Here, the relationship is assessed regarding the SF densities. The relationship is examined in terms of the Silk-Elmegreen law. Here, 4 density thresholds like 0.0, 0.05, 100, and 1000 cm-3 are considered. Every density-varying case is close to the dashed black line. As per the analysis, the proper choice of parameters aids in fitting the zero point of the star formation law.

C. Strength Assessment

The strength assessment refers to the strength and influence of stellar bars in the galaxy. Here, the star formation's strength is evaluated.

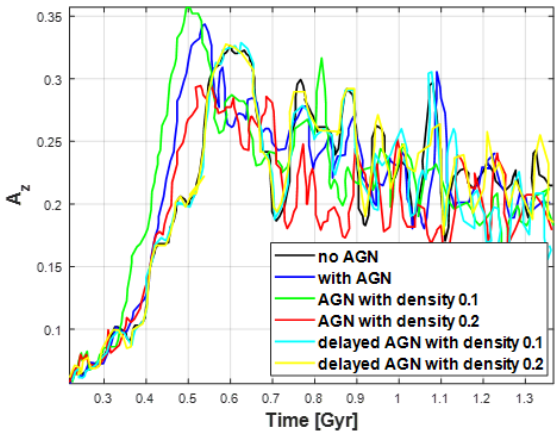

Fig. 5.

The strength (A_z) vs time analysis of star formation is displayed in Figure 5. The stellar bar's strength can considerably impact on the dynamics and evolution of galaxies, encompassing their star formation processes. Here, while considering AGN feedback, AGN feedback with a density of 0.1, and AGN feedback with a density of 0.2, the bar grows quicker as well as the bar strength's peak value is attained formerly. Therefore, the analysis displays that taking AGN feedback into account yields more strength in the spiral galaxy's star formation.

D. Mass Assessment

Here, the gas masses in the central region as well as the black hole masses are examined.

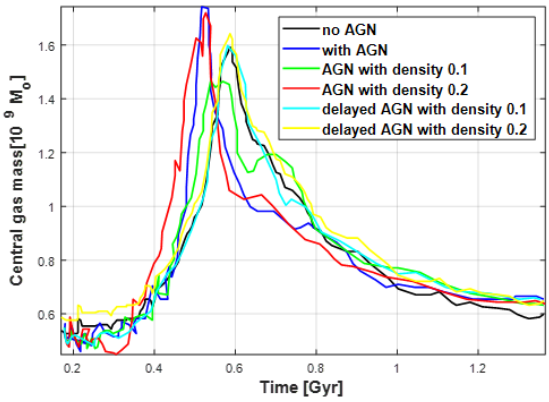

Fig. 6.

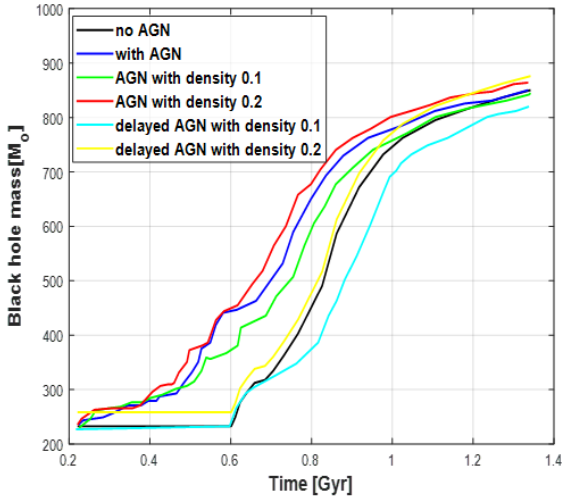

Fig. 7.

Figure 6 examines the mass analysis regarding the collected J0313–1806 astronomical data as well as the extracted factors by covered theories in this research framework. Here, the mass values are changed according to the time. The gas mass assessment shows that the central region with AGN, AGN with a density of 0.1, and AGN with a density of 0.2 attained higher gas mass as well as black hole mass. The performance varied according to time. Thus, the bar is formed formerly in simulations with AGN feedback; thus, the central gas density is allowed to build up more quickly.

In Table 1, the overall central gas mass and black hole mass assessment are displayed. Here, the AGN feedback mechanism with density achieved the central gas mass of 0.369 as well as the black hole mass of 0.188 for AGN with a 0.1 density. The AGN with density 0.2 had 0.361 mass of central gas as well as 0.185 mass of black hole. The mass value changes according to

Table 1
Central gas mass and black hole mass assessment

Star formation mechanism	Mass of central gas	Mass of black hole
No AGN	0.409	0.212
With AGN	0.387	0.192
AGN with density 0.1	0.369	0.188
AGN with density 0.2	0.361	0.185
Delayed AGN with density 0.1	0.398	0.196
Delayed AGN with density 0.2	0.400	0.208

the AGN mechanism.

E. SFR Analysis

A measure of the amount of mass of stars formed per unit time is known as SFR. Here, the SFR is examined for global and central star formation.

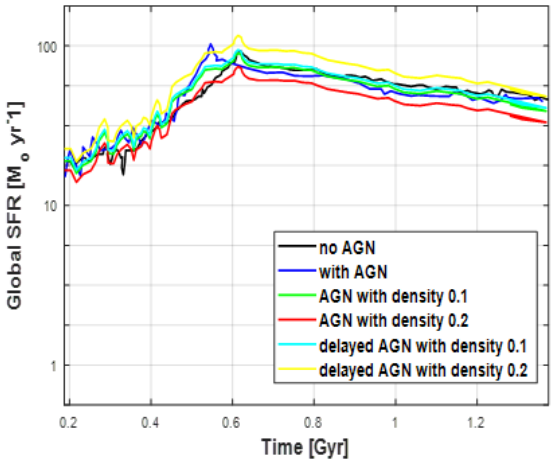

Fig. 8.

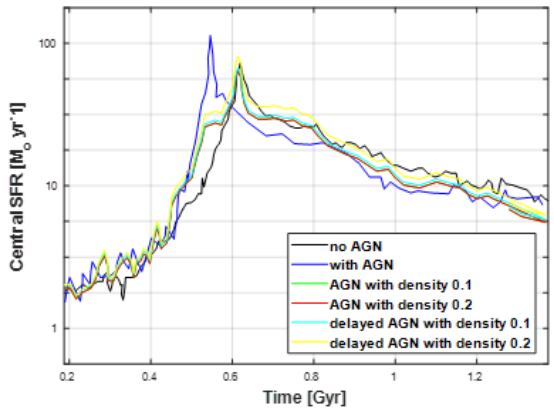

Fig. 9. SFR analysis for global and central

The SFR analysis for global and central is assessed in Figure 9. The global SFR slowly drops over time, and it isn't impacted by feedback. The central SFR gradually elevates and is presented more irregularly. In the central SFR analysis, the feedback is influenced. Hence, there is SFR while following the AGN feedback since it follows both radiative and mechanical feedback.

6. Conclusion

This research presents a detailed analysis of the SF and feedback mechanism in spiral galaxies. The spiral's structure is analyzed in the research framework based on the central gas, black hole, and SFR factors. The AGN feedback mechanism with density acquired the central gas mass of 0.369 as well as the black hole mass of 0.188 for AGN with a density of 0.1. Moreover, the SFR was higher while considering the AGN feedback mechanism. Also, by using the Silk-Elmegreen law, the relationship betwixt the SFR and surface density of gas in a spiral galaxy was assessed. The hydrodynamic analysis shows that the DIG had a higher fraction of contribution. As per the overall analysis, the star formation was positively influenced by the feedback mechanism. Nevertheless, it was challenging to trace the entire star formation across diverse phases.

Future Scope: The research work will be enhanced in the future with advanced laws and procedures to trace the entire star formation as well as the feedback mechanism in spiral galaxies.

References

[1] C. J. Aouad, P. A. James, and I. V. Chilingarian, "Coupling local to global star formation in spiral galaxies: The effect of differential rotation," *Mon. Not. R. Astron. Soc.*, vol. 496, no. 4, pp. 5211-5226, Jul. 2020.

[2] F. Calura et al., "Sub-parsec resolution cosmological simulations of star-forming clumps at high redshift with feedback of individual stars," *Mon. Not. R. Astron. Soc.*, vol. 516, no. 4, pp. 5914-5934, Nov. 2022.

[3] S. Dye et al., "The UKIRT Hemisphere Survey: Definition and J-band data release," *Mon. Not. R. Astron. Soc.*, vol. 473, no. 4, pp. 5113-5125, Jan. 2018.

[4] R. Feldmann, "The link between star formation and gas in nearby galaxies," *Commun. Phys.*, vol. 3, no. 1, pp. 1-10, June 2020.

[5] A. Fraser-McKelvie et al., "SDSS-IV MaNGA: The link between bars and the early cessation of star formation in spiral galaxies," *Mon. Not. R. Astron. Soc.*, vol. 499, no. 1, pp. 1116-1125, Oct. 2020.

[6] M. Frosst et al., "The diversity of spiral galaxies explained," *Mon. Not. R. Astron. Soc.*, vol. 514, no. 3, pp. 3510-3531, Aug. 2022.

[7] S. Gillman et al., "From peculiar morphologies to Hubble-type spirals: The relation between galaxy dynamics and morphology in star-forming galaxies at z ~ 1.5," *Mon. Not. R. Astron. Soc.*, vol. 492, no. 1, pp. 1492-1512, Feb. 2020.

[8] R. Guo et al., "Toward an understanding of the massive red spiral galaxy formation," *Astrophys. J.*, vol. 897, no. 2, pp. 1-16, July 2020.

[9] T. H. Jarrett et al., "A new Wide-field Infrared Survey Explorer calibration of stellar mass," *Astrophys. J.*, vol. 946, no. 2, pp. 1-14, Feb. 2023.

[10] W.-T. Kim, C.-G. Kim, and E. C. Ostriker, "Local simulations of spiral galaxies with the TIGRESS framework. I. Star formation and arm spurs/feathers," *Astrophys. J.*, vol. 898, no. 1, pp. 1-30, July 2020.

[11] C. Lammers et al., "Active galactic nuclei feedback in SDSS-IV MaNGA: AGNs have suppressed central star formation rates," *Astrophys. J.*, vol. 953, no. 1, pp. 1-17, Sept. 2023.

[12] B. Margalef-Bentabol et al., "Observations of the initial formation and evolution of spiral galaxies at $1 < z < 3$ in the CANDELS field," *Mon. Not. R. Astron. Soc.*, vol. 511, no. 1, pp. 1502-1517, Feb. 2022.

[13] S. Meingast et al., "VISIONS: The VISTA Star Formation Atlas: I. Survey overview," *Astron. Astrophys.*, vol. 673, pp. 1-14, May 2023.

[14] N. P. H. Nesvadba et al., "Jet-driven AGN feedback on molecular gas and low star-formation efficiency in a massive local spiral galaxy with a bright X-ray halo," *Astron. Astrophys.*, vol. 654, pp. 1-18, Oct. 2021.

[15] E. C. Ostriker and C.-G. Kim, "Pressure-regulated, feedback-modulated star formation in disk galaxies," *Astrophys. J.*, vol. 936, no. 2, pp. 1-26, Aug. 2022.

[16] A. Prieto et al., "The PARSEC view of star formation in galaxy centres: From protoclusters to star clusters in an early-type spiral," *Mon. Not. R. Astron. Soc.*, vol. 533, no. 1, pp. 433-454, Jan. 2024.

[17] S. Rieder et al., "The formation and early evolution of embedded star clusters in spiral galaxies," *Mon. Not. R. Astron. Soc.*, vol. 509, no. 4, pp. 6155-6168, Jan. 2022.

[18] V. A. Semenov, A. V. Kravtsov, and N. Y. Gnedin, "Spatial decorrelation of young stars and dense gas as a probe of the star formation-feedback cycle in galaxies," *Astrophys. J.*, vol. 918, no. 1, pp. 1-19, Sept. 2021.

[19] S. J. Smartt et al., "GW190425: Pan-STARRS and ATLAS coverage of the skymap and limits on optical emission associated with FRB 20190425A," *Mon. Not. R. Astron. Soc.*, pp. 1-9, Jan. 2023.

[20] M. V. Smith et al., "A multiwavelength study of star formation in 15 local star-forming galaxies," *Mon. Not. R. Astron. Soc.*, vol. 505, no. 3, pp. 3998-4035, July 2021.

[21] S. E. Tuttle and S. Tonnesen, "BreakBRD galaxies. I. Global properties of spiral galaxies with central star formation in red disks," *Astrophys. J.*, vol. 889, no. 2, pp. 1-14, Feb. 2020.

[22] M. Valentini et al., "Impact of H2-driven star formation and stellar feedback from low-enrichment environments on the formation of spiral galaxies," *Mon. Not. R. Astron. Soc.*, vol. 518, no. 1, pp. 1128-1147, Jan. 2023.

[23] H. Xu et al., "DESI Legacy Imaging Surveys Data Release 9: Cosmological constraints from galaxy clustering and weak lensing using the minimal bias model," *Sci. China Phys. Mech. Astron.*, vol. 66, no. 12, pp. 1-24, Dec. 2023.

[24] J. Yang et al., "Pōniuā‘ena: A luminous z = 7.5 quasar hosting a 1.5 billion solar mass black hole," *Astrophys. J. Lett.*, vol. 897, no. 1, pp. 1-9, July 2020.

[25] S. Y. Yu, L. C. Ho, and J. Wang, "Spiral structure boosts star formation in disk galaxies," *Astrophys. J.*, vol. 917, no. 2, pp. 1-9, Aug. 2021.

[26] S. Zhou et al., "Star formation histories of massive red spiral galaxies in the local universe," *Astrophys. J.*, vol. 916, no. 1, pp. 1-13, July 2021.